Macromolecules

Article

pubs.acs.org/Macromolecules

Extending π-Conjugation System with Benzene: An Effective Method To Improve the Properties of Benzodithiophene-Based Polymer for Highly Efficient Organic Solar Cells

Jiuxing Wang,[†,‡] Manjun Xiao,[†,§] Weichao Chen,[†] Meng Qiu,[†] Zhengkun Du,[†] Weiguo Zhu,[§] Shuguang Wen,[†] Ning Wang,[†] and Renqiang Yang*[,†,∥]

[†]CAS Key Laboratory of Bio-based Materials, Qingdao Institute of Bioenergy and Bioprocess Technology, Chinese Academy of Sciences, Qingdao 266101, China

[‡]University of Chinese Academy of Sciences, Beijing 100049, China

[§]College of Chemistry, Key Lab of Environment-Friendly Chemistry and Application of the Ministry of Education, Xiangtan University, Xiangtan 411105, China

[∥]State Key Laboratory of Luminescent Materials and Devices, South China University of Technology, Guangzhou 510641, China

Supporting Information

ABSTRACT: To obtain a polymer based on benzodithiophene (BDT) owning both a largely extended π-conjugation system and a low-lying highest occupied molecular orbital (HOMO), a polymer (PBDTBzT-DTffBT) containing benzothienyl-substituted BDT is designed and synthesized. Compared with the polymer (PBDTT-DTffBT) based on thienyl-substituted BDT, PBDTBzT-DTffBT exhibits better thermal stabilities, red-shifted absorption spectra, and stronger intermolecular interactions. The HOMO and lowest unoccupied molecular orbital (LUMO) in PBDTBzT-DTffBT are decreased by 0.11 and 0.13 eV, respectively, which should be attributed to the contribution of the electron-withdrawing group benzene. Polymer solar cells (PSCs) based on PBDTBzT-DTffBT and [6,6]-phenyl-C_{61}-butyric acid methyl ester ($PC_{61}BM$) exhibit a maximum power conversion efficiency (PCE) of 7.30% with a large open-circuit voltage of 0.90 V under AM 1.5G illumination (100 mW/cm^2). The PCE is 36% higher than that of the PSCs derived from PBDTT-DTffBT. These findings provide a new approach to design high-performance conjugated polymers for efficient solution-processed PSCs.

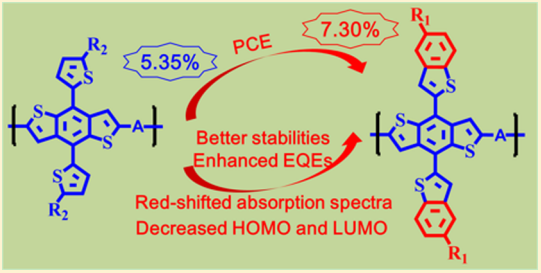

1. INTRODUCTION

With the development of the society and the explosion of the population, global energy demand is increasing. As the solar energy alone could in principle meet the rising demand for energy, photovoltaics have attracted considerable attention of researchers.[1] Significant progress has been made in bulk heterojunction polymer solar cells (BHJ-PSCs), and power conversion efficiencies (PCEs) of over 9% have been achieved for single PSCs in the past 10 years.[2−6] Since [6,6]-phenyl-C_{71}-butyric acid methyl ester ($PC_{71}BM$) and [6,6]-phenyl-C_{61}-butyric acid methyl ester ($PC_{61}BM$) are currently the most efficient and widely used electron acceptors, development of conjugated polymer donor materials plays a vital role in achieving high-performance PSCs.[7−16] The PCE (PCE = $V_{oc} \times J_{sc} \times FF/P_{in}$) is related to the open-circuit voltage (V_{oc}), short-circuit current (J_{sc}), and fill factor (FF) values.[17] To achieve a high PCE, an ideal conjugated polymer should possess suitable energy levels and good solubility.[18−21] Alternating the electron-rich donor (D) and electron-deficient acceptor (A) units in the backbone of the polymer is currently the most popular and successful strategy to design high-performance polymer donor materials.[19−21]

Alkylthienyl-substituted benzodithiophene (BDTT) is a promising building block for constructing high-performance D−A conjugated polymers. Extensive research focused on BDTT has been carried out to improve the photovoltaic properties of BDTT-based polymers.[9,13,22,23] Extending π-conjugation system is normally an effective way to obtain high-performance polymers, since the largely extended π-conjugation system could enhance π-electron delocalization, thus facilitating to improve their photovoltaic properties.[24−30] In 2013, Hou and co-workers synthesized a polymer containing alkylthienyl-substituted dithienobenzodithiophene (DTBDTT).[31] The PSCs based on DTBDTT showed a maximum PCE of 7.79%, which was 31% higher than that of the PSCs based on BDTT. Recently, Hwang et al. reported a new BDT monomer (BDTTT) by introducing two thieno[3,2-*b*]thiophene (TT) groups onto the BDT unit.[26] The large π-conjugation system improved the molecular ordering of the

Received: August 26, 2014
Revised: October 22, 2014
Published: November 7, 2014

Scheme 1. Synthetic Routes of BDTBzT and the Polymers

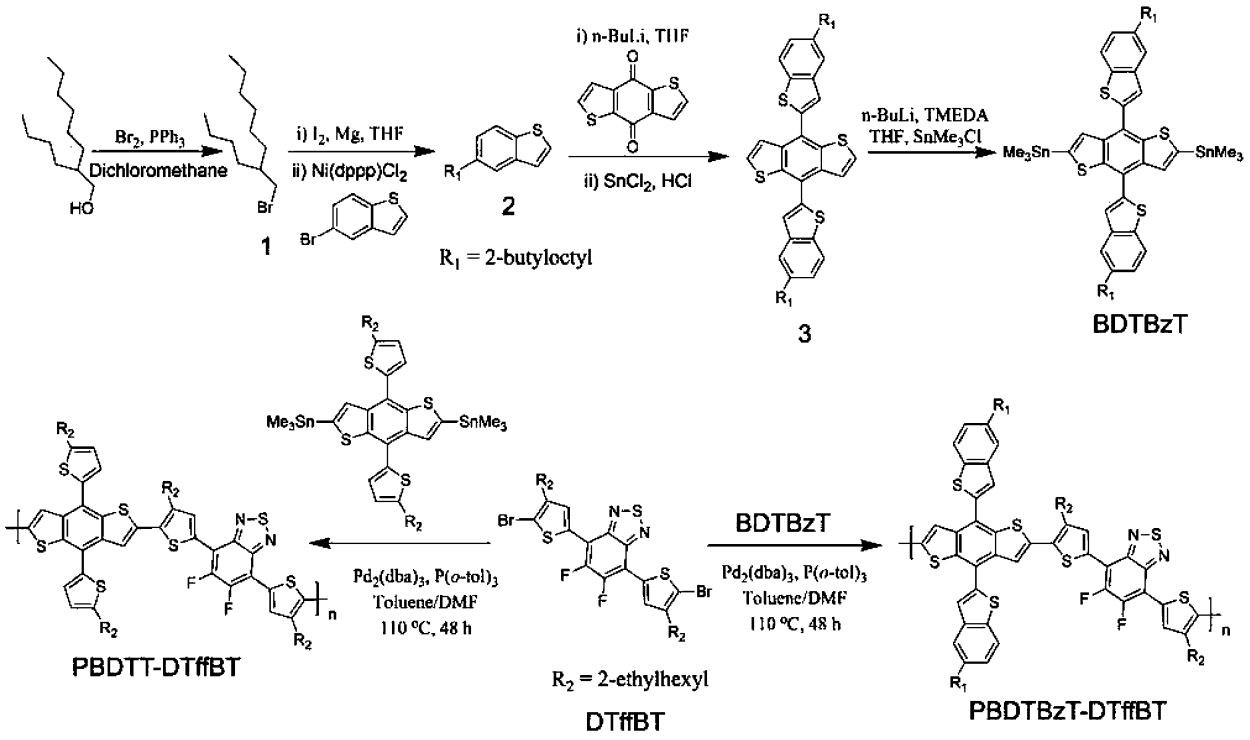

polymer. The PCE reached 7.44% for conventional PSCs and 7.71% for inverted PSCs.

However, polymers with a largely extended π-conjugation system exhibit a high-lying highest occupied molecular orbital (HOMO) energy level,[32−34] which is assumed to limit the V_{oc} in corresponding PSCs.[18] The HOMO energy levels of the polymers based on π-extended BDTT are in the range between −5.15 and −5.31 eV, leading to low V_{oc} values of below 0.80 V.[26,31,35] To obtain a polymer containing BDTT derivative simultaneously owning a largely extended π-conjugation system and a low-lying HOMO energy level, we designed a novel benzothienyl (BzT)-substituted BDT (BDTBzT) as the electron-rich donor unit. As we know, thiophene is a six-π-electron five-membered heteroaromatic compound while benzene is a six-π-electron six-membered aromatic compound. Compared with thiophene ring, benzene is π-deficient. When fused with benzene, the electron density in the thiophene ring would be decreased, which would lead to a lower-lying HOMO energy level. To further downshift the HOMO energy level of the polymer, 4,7-di((4-(2-ethylhexyl)-2-thienyl)-5,6-difluoro-2,1,3-benzothiadiazole (DTffBT) was chosen as the electron-deficient acceptor unit. Previous reports have shown that the two fluorine atoms on the DTffBT unit could pronouncedly downshift the HOMO energy level of the corresponding polymer.[36−39] Thus, the new conjugated polymer PBDTBzT-DTffBT comprising BDTBzT and DTffBT was synthesized. Another polymer PBDTT-DTffBT consisting of BDTT and DTffBT was prepared for comparison. The HOMO and lowest unoccupied molecular orbital (LUMO) energy levels in PBDTBzT-DTffBT were decreased by 0.11 and 0.13 eV, respectively, in comparison with those in PBDTT-DTffBT. The HOMO energy level of PBDTBzT-DTffBT was as low as −5.47 eV, leading to a high V_{oc} of 0.90 V. The PCE was sharply increased by 36%, from 5.35% to 7.30%. This PCE value is among the highest ones for $PC_{61}BM$-based PSCs without any electron transport layers.[7,14,38−40]

2. RESULTS AND DISCUSSION

Synthesis and Characterization of the Polymer. Synthetic routes of BDTBzT, PBDTBzT-DTffBT, and PBDTT-DTffBT are shown in Scheme 1. Detailed experimental procedures for the synthesis of the monomers and polymers are given in the Experimental Section. Compound **1**, BDTT, and DTffBT were synthesized according to reported methods.[10,38,41] The two polymers were prepared by Stille coupling reaction with tris(dibenzylideneacetone)dipalladium ($Pd_2(dba)_3$) and tri(*o*-tolyl)phosphine ($P(o\text{-tol})_3$) as catalysts. Both of the polymers showed a limited solubility in common solvents at room temperature. Fortunately, they could be dissolved in *o*-dichlorobenzene (DCB) at 90 °C. Gel permeation chromatography (GPC) was used to measure the number-average molecular weights (M_n) of the polymers. The M_n of PBDTBzT-DTffBT and PBDTT-DTffBT were found to be 22 and 24 kDa, with a polydispersity index (PDI) of 1.84 and 1.20, respectively.

The thermal stability of the polymers was analyzed by thermogravimetric analysis (TGA) with a heating rate of 10 °C/min under a nitrogen atmosphere. Figure 1 shows the TGA plots of the two polymers. The thermal decomposition temperatures (5% weight loss) of PBDTBzT-DTffBT and PBDTT-DTffBT were 441 and 431 °C, respectively. By fusing benzene on the flanking thiophene ring of BDTT, the thermal stability of the corresponding polymer was enhanced.

Optical Properties. Figure 2a shows the absorption spectra of the two polymers in dilute DCB solution and as thin films. Detailed absorption data are listed in Table 1. Compared with the control polymer, PBDTBzT-DTffBT showed similar but red-shifted absorption bands. The main absorption peak of PBDTBzT-DTffBT at 602 nm in solution arose from

dx.doi.org/10.1021/ma501756p | Macromolecules 2014, 47, 7823−7830

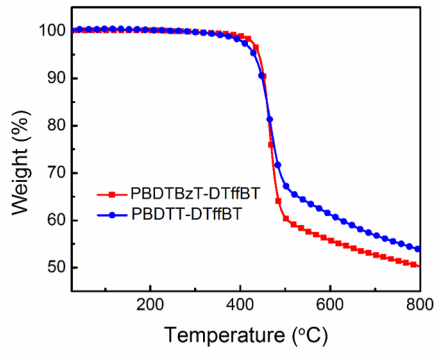

Figure 1. TGA plots of PBDTBzT-DTffBT and PBDTT-DTffBT.

intramolecular charge transfer (ICT) while the absorption peaks in shorter-wavelength region should be assigned to localized $\pi-\pi^*$ transitions.[14,42] The shoulder peak in the long wavelength could be attributed to intermolecular $\pi-\pi^*$ transitions due to the aggregations of the polymer chains.[40,43] The shoulder peak of PBDTBzT-DTffBT was more distinct than that of the control polymer, indicating that intermolecular interactions were enhanced when benzene fused on the thiophene ring. From solution to solid state, the main absorption peak of PBDTBzT-DTffBT was red-shifted by 14 nm, and the intensity of the shoulder peak was increased due to stronger intermolecular interactions in the solid state. When benzene fused on the flanking thiophene ring, the absorption edge of PBDTBzT-DTffBT film moved from 702 to 713 nm. The optical bandgap (E_g^{opt}) of PBDTBzT-DTffBT calculated from the absorption edge was 1.74 eV, which was decreased by 0.02 eV in comparison with that of the control polymer (1.76 eV). Thus, a larger J_{sc} could be expected for PBDTBzT-DTffBT-based PSCs.

Figure 2b shows the absorption spectra of PBDTBzT-DTffBT in DCB solution under different temperatures. With increasing the temperature, the intensity of the shoulder was declined because the aggregations weakened.[40] Meanwhile, the absorption spectra were blue-shifted gradually as the backbone of the polymer was becoming more twisting with the rising temperature.[44] Unexpectedly, the intensity of the absorption peak at 428 nm also declined and finally disappeared during the heating process. This phenomenon implied that the absorption peak at 428 nm also arose from the aggregations of the polymer chains. Despite the strong aggregation ability of PBDTBzT-DTffBT, the X-ray diffraction (XRD) spectrum (Figure S1, Supporting Information) of the polymer film showed no crystalline peaks, implying that the aggregated polymer film was still amorphous.

Electrochemical Properties. Cyclic voltammetry (CV) was used to investigate the electrochemical properties of the polymers.[45] The cyclic voltammetric curves and the energy levels of the polymers are shown in Figure 3. The onset oxidation potentials (E_{ox}) of PBDTBzT-DTffBT and PBDTT-DTffBT were 1.06 and 0.95 V vs saturated calomel electrode (SCE), respectively. In this work, the half-wave potential of the ferrocene/ferrocenium (Fc/Fc) redox couple ($E_{1/2,(Fc/Fc^+)}$) was measured to be 0.39 V vs SCE. According to the equation $E_{HOMO} = -e(E_{ox} + 4.8 - E_{1/2,(Fc/Fc^+)})$,[46] the HOMO energy levels of PBDTBzT-DTffBT and PBDTT-DTffBT were −5.47 and −5.36 eV, respectively, as shown in Table 1. The HOMO energy level of PBDTBzT-DTffBT was downshifted by 0.11 eV in comparison with that of the control polymer. The decrease of the HOMO energy level of PBDTBzT-DTffBT should be attributed to the contribution of the electron-withdrawing group benzene. To the best of our knowledge, this is the deepest HOMO energy level for the polymers based on π-extended BDTTs.[26,31,35] The LUMO energy levels of PBDTBzT-DTffBT and PBDTT-DTffBT were −3.73 and −3.60 eV, respectively, calculated from the equation $E_{LUMO} = E_{HOMO} + E_g^{opt}$. The LUMO of PBDTBzT-DTffBT was downshifted by 0.13 eV. These results clearly indicated that fusing benzene on the flanking thiophene ring of BDTT could simultaneously downshift the HOMO and LUMO energy levels in the corresponding polymer.

Theoretical Calculations. The energies and distributions of the frontier molecular orbitals of PBDTT-DTffBT and PBDTBzT-DTffBT were investigated by density functional theory (DFT) using the Gaussian 09 program at the B3LYP/6-31G(d,p) level in the gas phase. The optimized molecular geometries were confirmed to be minimum-energy conformations by computing vibrational frequencies at the same level. In this work, one repeat unit was chosen, and alkyl chains were simplified into methyl groups to reduce the calculation time. The results are shown in Table 1 and Figure S2. Compared with PBDTT-DTffBT, PBDTBzT-DTffBT showed a lower-lying HOMO and LUMO, which was consistent with the results obtained from cyclic voltammetry. The two polymers showed similar distributions of the frontier molecular orbitals. The HOMO was delocalized over the whole backbone while the LUMO was mainly located in the DTffBT unit.

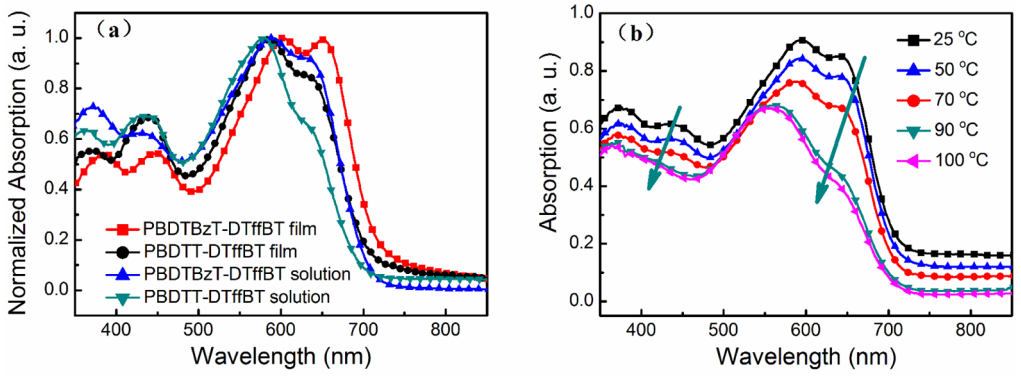

Figure 2. Absorption spectra of (a) PBDTBzT-DTffBT and PBDTT-DTffBT in DCB solution and as thin films and (b) PBDTBzT-DTffBT in DCB solution under different temperatures.

dx.doi.org/10.1021/ma501756p | Macromolecules 2014, 47, 7823−7830

Table 1. Optical Absorption Properties and Molecular Energy Levels of the Polymers

polymer	λ_{max} (nm) solution	λ_{max} (nm) film	λ_{edge} (nm)	HOMO[a] (eV)	LUMO[b] (eV)	E_g^{opt} [c] (eV)	HOMO[d] (eV)	LUMO[d] (eV)
PBDTBzT-DTffBT	370, 428, 588	386, 448, 602, 652	713	−5.47	−3.73	1.74	−5.12	−2.80
PBDTT-DTffBT	362, 430, 579	364, 438, 585	702	−5.36	−3.60	1.76	−5.08	−2.79

[a]Measured by cyclic voltammetry. [b]Calculated from the equation $E_{LUMO} = E_{HOMO} + E_g^{opt}$. [c]Calculated from the absorption band edge of the polymer film. [d]Calculated via DFT.

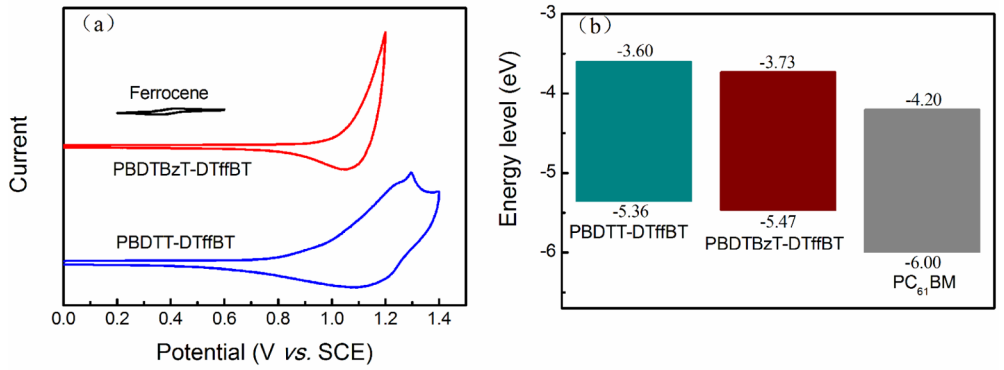

Figure 3. (a) Cyclic voltammograms and (b) HOMO and LUMO energy levels of the polymers.

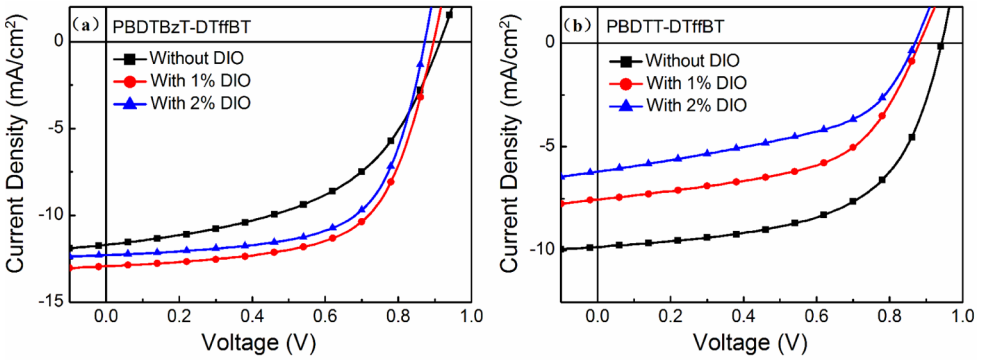

Figure 4. *J*–*V* curves of the PSCs based on (a) PBDTBzT-DTffBT and (b) PBDTT-DTffBT with different DIO additive amounts.

Photovoltaic Properties and Morphology Characterization. Conventional BHJ-PSC devices were fabricated with a typical structure of indium tin oxide (ITO)/poly(3,4-ethylenedioxythiophene):poly(styrenesulfonate) (PEDOT:PSS)/polymer:$PC_{61}BM$/Ca/Al. The polymer and $PC_{61}BM$ were dissolved in DCB at 90 °C. The thickness of the active layer in this work was ∼90 nm. Different donor/acceptor (D/A) ratios (w/w) and DIO additive amounts (v/v) were investigated to optimize the photovoltaic performance of the polymers. The optimal D/A ratios were 1.5:1 and 1:1 for the PSCs based on PBDTBzT-DTffBT and PBDTT-DTffBT, respectively (Table S1 and Figure S3). The current density–voltage (*J*–*V*) curves of the optimized PSCs with different DIO additive amounts are shown in Figure 4. The detailed photovoltaic parameters are summarized in Table 2.

Without any processing additives or post-treatments, the PSCs based on PBDTT-DTffBT showed a maximum PCE of 5.35% with a V_{oc} = 0.94 V and a J_{sc} = 9.83 mA/cm^2 while the PSCs derived from PBDTBzT-DTffBT exhibited a similar PCE value of 5.33% with a V_{oc} of 0.91 V and a J_{sc} of 11.68 mA/cm^2. When treated with DIO additive, the photovoltaic properties of PBDTBzT-DTffBT were greatly enhanced while those of the control polymer sharply deteriorated. Processed with 1% DIO additive, the PSCs based on PBDTT-DTffBT exhibited a low PCE of 3.61%, with a V_{oc} = 0.88 V, a J_{sc} = 7.55 mA/cm^2, and an FF = 54.29%. Under the same conditions, a maximum PCE of 7.30% with a high V_{oc} = 0.90 V, a large J_{sc} = 12.93 mA/cm^2, and an FF = 62.73% was obtained for PBDTBzT-DTffBT. The V_{oc} of 0.90 V was lower than that (0.94 V) of the best performing PSCs derived from PBDTT-DTffBT despite that PBDTBzT-

Table 2. Photovoltaic Properties of the PSCs with a Conventional Structure of ITO/PEDOT:PSS/Polymer:$PC_{61}BM$/Ca/Al under AM 1.5G Illumination (100 mW/cm^2)

polymer	DIO (%)	V_{oc} (V)	J_{sc} (mA/cm^2)	FF (%)	PCE_{max} (PCE_{ave})[a] (%)
PBDTBzT-DTffBT	0	0.91	11.68	50.19	5.33 (5.17)
	1	0.90	12.93	62.73	7.30 (7.16)
	2	0.87	12.28	63.71	6.81 (6.65)
PBDTT-DTffBT	0	0.94	9.83	57.91	5.35 (5.32)
	1	0.88	7.55	54.29	3.61 (3.42)
	2	0.87	6.19	48.47	2.61 (2.50)

[a]The average PCE was obtained from five devices.

dx.doi.org/10.1021/ma501756p | Macromolecules 2014, 47, 7823–7830

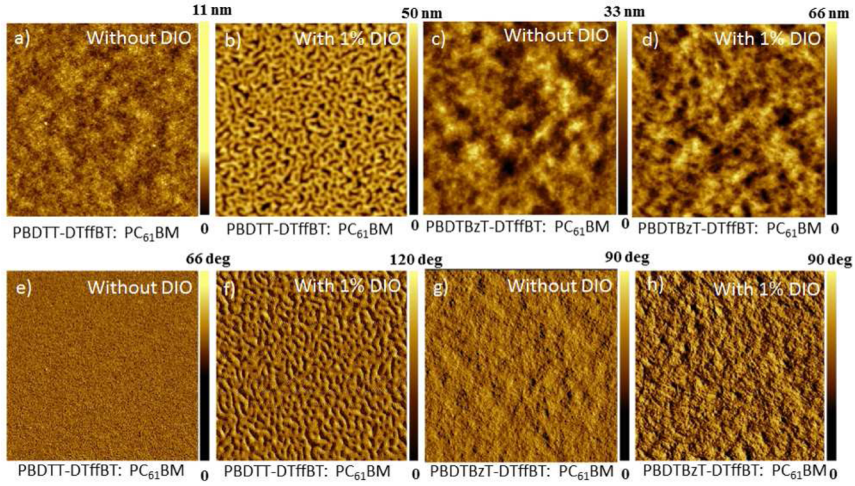

Figure 5. AFM (a–d) topography and (e–h) phase images of the PBDTT-DTffBT:$PC_{61}BM$ (1:1) and PBDTBzT-DTffBT:$PC_{61}BM$ (1.5:1) blend films processed without or with 1% DIO additive. The size of the images is 5 μm × 5 μm.

DTffBT exhibited a deeper HOMO. In addition to the difference between the HOMO of the donor and the LUMO of the acceptor, other factors such as saturation dark current density, recombination dynamics, shunt resistance, and morphology can also affect the V_{oc}.[34,47−51] Although the V_{oc} for PBDTBzT-DTffBT is lower than that for PBDTT-DTffBT, to the best of our knowledge, it is still the highest one for the PSCs based on π-extended BDTT.[26,31,35] The red-shifted absorption of PBDTBzT-DTffBT, which covered a higher fraction of the sunlight (Figure 2a), could be considered as a contributing factor of the improvement of the J_{sc} for PBDTBzT-DTffBT. The PCE of 7.30% is among the highest ones for $PC_{61}BM$-based PSCs without any electron transport layer modifications.[7,14,38−40] Thus, fusing benzene on the flanking thiophene ring of BDTT greatly improved the photovoltaic properties of the corresponding polymer.

Solvent additives play an important role in morphology control in PSCs.[52] Atomic force microscopy (AFM) was used to explore the effects of DIO additive on the surface morphology of active layers.[53] Figure 5 shows the topography and phase images of the PBDTT-DTffBT:$PC_{61}BM$ (1:1) and PBDTBzT-DTffBT:$PC_{61}BM$ (1.5:1) blend films processed without or with 1% DIO additive. The surface of the PBDTT-DTffBT:$PC_{61}BM$ film obtained without DIO was very smooth with a root-mean-square (RMS) surface roughness of 0.45 nm (Figure 5a). When processed with 1% DIO, the film formed a much rougher surface topography (RMS = 7.59 nm) with dramatically aggregated domains (Figure 5b). For the PBDTBzT-DTffBT:$PC_{61}BM$ film, the addition of 1% DIO also resulted in a rougher surface topography but without large domains (Figure 5c,d). The RMS was increased from 4.69 to 8.25 nm, suggesting appropriately enhanced aggregations at the surface.[54] The above AFM results revealed that the addition of 1% DIO additive led to a deteriorated surface morphology of PBDTT-DTffBT:$PC_{61}BM$ and an improved surface morphology of PBDTBzT-DTffBT:$PC_{61}BM$, which were consistent with the device performance.[11,27,52,55,56]

Figure 6 exhibits the external quantum efficiency (EQE) curves of the optimized PSCs based on PBDTBzT-DTffBT and PBDTT-DTffBT. One can observe that the EQE curves well matched their absorption spectra. The PSCs derived from PBDTBzT-DTffBT showed a more efficient photoresponse across the whole spectrum, which indicated that fusing benzene

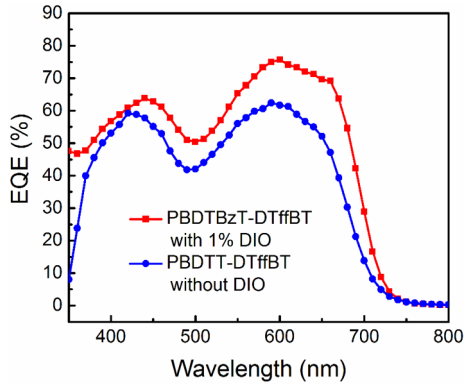

Figure 6. EQE curves of the PSCs based on PBDTT-DTffBT:$PC_{61}BM$ (1:1) and PBDTBzT-DTffBT:$PC_{61}BM$ (1.5:1).

on the flanking thiophene ring could enhance the current density. Therefore, the J_{sc} for PBDTBzT-DTffBT was improved greatly. The J_{sc} integrated from the EQE curves were 12.79 and 9.95 mA/cm^2 for PBDTBzT-DTffBT and PBDTT-DTffBT-based devices, respectively, which were quite consistent with those obtained from the J–V curves.

3. CONCLUSIONS

In conclusion, we have provided an effective method to improve the properties of the polymer based on BDTT by extending the π-conjugation system with benzene. Fusing benzene on the flanking thiophene ring of BDTT could slightly red-shift the absorption bands, obviously enhance the intermolecular interactions, and pronouncedly downshift the HOMO and LUMO energy levels. As a result, the photovoltaic properties of PBDTBzT-DTffBT are improved greatly. The optimized PSCs exhibit a high PCE of 7.30%, which is among the highest ones for $PC_{61}BM$-based PSCs without any electron transport layer modifications. This work provides a new approach to design largely π-extended polymers for high-performance PSCs.

4. EXPERIMENTAL SECTION

Materials. All reagents were purchased from J&K Scientific and other commercial sources. The reagents were used directly unless otherwise noted. Tetrahydrofuran (THF) and toluene were dried over

dx.doi.org/10.1021/ma501756p | Macromolecules 2014, 47, 7823−7830

sodium, and *N*,*N*-dimethylformamide (DMF) was dried over calcium hydride. Compound **1**, BDTT, and DTffBT were synthesized according to reported procedures.[10,38,41] BDTBzT and the two polymers were synthesized according to Scheme 1. Synthetic details are described below.

Measurements. ^{1}H NMR and ^{13}C NMR spectra were recorded using a Bruker DRX-600 spectrometer with tetramethylsilane (TMS) as an internal standard. High-resolution mass spectra (HRMS) were performed on a Bruker Maxis UHR-TOF under APCI mode. UV−vis absorption spectra were obtained on a Hitachi U-4100 spectrophotometer. The molecular weights of the polymers were measured by GPC using THF as the solvent and polystyrene as the standard under 40 °C. TGA was performed on a SDT Q600 with a heating rate of 10 °C/min under a nitrogen atmosphere. CV was measured on a CHI660D electrochemical workstation in a solution of tetrabutylammonium hexafluorophosphate (Bu_4NPF_6, 0.1 M) in acetonitrile at a scan rate of 100 mV/s. The three-electrode system was composed of Pt electrode coated with the sample film as the working electrode, Pt wire as the counter electrode, and SCE as the reference electrode. DFT calculations were carried out by the Gaussian 09 program suite at the B3LYP/6-31G(d,p) level in the gas phase. The optimized molecular geometries were confirmed to be minimum-energy conformations by computing vibrational frequencies at the same level. AFM measurements were performed using an Agilent 5400 in tapping mode under ambient conditions. The XRD spectrum was obtained on a Hitachi S-4800.

Fabrication of Photovoltaic Devices. Conventional BHJ-PSC devices were fabricated with the configuration of ITO/PEDOT:PSS/polymer:$PC_{61}BM$/Ca/Al. The ITO-coated glasses with a nominal sheet resistance of 15 Ω/sq were cleaned in an ultrasonic bath with detergent, ultrapure water, acetone, and isopropyl alcohol subsequently. After a 10 min oxygen plasma treatment, a thin layer of PEDOT:PSS (30 nm) was spin-coated onto the ITO anode and then dried at 160 °C for 20 min. The polymer and $PC_{61}BM$ (30 mg/mL) were dissolved in DIO/DCB (0%, 1%, or 2%, v/v) solution. The solution was heated to 90 °C for 90 min before being spin-coated on the ITO/PEDOT:PSS electrode. The thickness of the active layer was ∼90 nm. Finally, 10 nm Ca and 100 nm Al layers were successively thermal evaporated onto the active layer at a pressure of 4.0×10^{-4} Pa. The active area of the device in this work was 0.1 cm^2. The current density−voltage (*J*−*V*) characteristics were recorded with a Keithley 2420 source measurement under AM 1.5G illumination (100 mW/cm^2) from a Newport solar simulator. A standard silicon solar cell was used to calibrate the light intensity. The external quantum efficiencies (EQE) of the PSCs were measured using a certified Newport incident photon conversion efficiency (IPCE) measurement system.

Synthetic Procedures. *Synthesis of 5-(2-Butyloctyl)benzo[b]-thiophene (**2**).* To a mixture of magnesium (2.05 g, 84.34 mmol), anhydrous THF (40 mL), and a small amount of iodine, 5-(bromomethyl)undecane (10.51 g, 42.17 mmol) in anhydrous THF (10 mL) was added dropwise at 60 °C under an argon atmosphere. The reaction mixture was refluxed for 2 h. Then the temperature was allowed to cool to room temperature. The solution was added dropwise to a mixture of 5-bromobenzo[*b*]thiophene (5.99 g, 28.11 mmol), [1,3-bis(diphenylphosphino)propane]dichloronickel(II) (Ni(dppp)$_2$Cl$_2$, 0.61 g, 1.12 mmol), and anhydrous THF (50 mL) at 0 °C. Then the temperature was increased to room temperature and stirred for 24 h. The mixture was quenched with 80 mL of saturated NH_4Cl and stirred for 10 min. Then the mixture was washed with saturated NH_4Cl (3×, 100 mL) and brine (1×, 100 mL). The crude product was dried with Na_2SO_4 and further purified by column chromatography using petroleum ether (PE) as the eluent to give a colorless liquid (4.46 g, 52.45% yield). ^{1}H NMR (600 MHz, $CDCl_3$): δ 7.78 (d, 1H), 7.60 (s, 1H), 7.41 (d, 1H), 7.29 (d, 1H), 7.17−7.15 (dd, 1H), 2.65 (d, 2H), 1.70−1.67 (m, 1H), 1.36−1.25 (m, 16H), 0.90−0.87 (m, 6H). ^{13}C NMR (150 MHz, $CDCl_3$): δ 139.93, 138.12, 137.19, 126.33, 126.24, 123.97, 123.79, 122.07, 40.63, 40.09, 33.27, 32.97, 32.07, 29.85, 28.99, 26.71, 23.22, 22.83, 14.31, 14.26. HRMS (APCI) *m*/*z* calcd for $C_{20}H_{31}S$ (MH^+) 303.2141; found 303.2169.

*Synthesis of 4,8-Bis(5-(2-butyloctyl)benzo[b]thiophen-2-yl)-benzo[1,2-b:4,5-b′]dithiophene (**3**).* Under the protection of argon, *n*-butyllithium (10.14 mL, 16.22 mmol, 1.6 M in hexane) was added dropwise to compound **2** (4.46 g, 14.75 mmol) in anhydrous THF (30 mL) at 0 °C. Then the mixture was warmed to 50 °C and stirred for 2 h. Benzo[1,2-*b*:4,5-*b*′]dithiophen-4,8-dione (1.08 g, 4.92 mmol) in anhydrous THF (15 mL) was added, and the mixture was stirred for 3 h at 70 °C. After cooling down to room temperature, $SnCl_2$ (7.46 g, 39.34 mmol) in 10% HCl (15 mL) was added, and the mixture was stirred overnight at 70 °C. After cooling to room temperature, the mixture was extracted by diethyl ether twice, and the combined organic phase was concentrated to obtain raw compound **3**. The crude product was purified by column chromatography using PE as the eluent to give a pale yellow solid. The product was further purified by recrystallization from ethyl acetate/isopropanol (v/v, 1/2). A pale yellow crystal was obtained (2.30 g, 59.08% yield). ^{1}H NMR (600 MHz, $CDCl_3$): δ 7.84 (d, 2H), 7.71 (d, 2H), 7.68 (s, 2H), 7.66 (s, 2H), 7.51 (d, 2H), 7.25−7.23 (dd, 2H), 2.70 (d, 4H), 1.74−1.72 (m, 2H), 1.38−1.28 (m, 32H), 0.93−0.88 (m, 12H). ^{13}C NMR (150 MHz, $CDCl_3$): δ 140.21, 140.05, 139.42, 138.72, 137.93, 136.94, 128.28, 126.83, 124.88, 124.49, 124.32, 123.39, 121.93, 40.71, 40.14, 33.30, 33.03, 32.09, 29.87, 29.03, 26.74, 23.26, 22.85, 14.35, 14.29. HRMS (APCI) *m*/*z* calcd for $C_{50}H_{63}S_4$ (MH^+) 791.3807; found 791.3804.

Synthesis of (4,8-Bis(5-(2-butyloctyl)benzo[b]thiophen-2-yl)-benzo[1,2-b:4,5-b′]dithiophene-2,6-diyl)bis(trime-thylstannane) (BDTBzT). To a mixture of compound **3** (1.10 g, 1.39 mmol), *N*,*N*,*N*′,*N*′-tetramethylethylenediamine (TMEDA, 0.62 mL, 4.13 mmol), and anhydrous THF (30 mL), *n*-butyllithium (2.35 mL, 3.76 mmol, 1.6 M in hexane) was added slowly at 0 °C under an argon atmosphere. The solution was stirred at 0 °C for 2 h, and then trimethyltin chloride (4.9 mL, 4.9 mmol, 1.0 M in THF) was added dropwise. The resulting mixture was stirred overnight at room temperature. The resulting solution was poured into 100 mL of cold water and extracted three times with diethyl ether. The organic layer was separated and dried over anhydrous Na_2SO_4. The solvent was removed, and the crude product was purified by recrystallization from acetone to obtain the target compound as a yellow solid (0.93 g, 59.91% yield). ^{1}H NMR (600 MHz, $CDCl_3$): δ 7.84 (d, 2H), 7.74 (t, 2H), 7.70 (s, 2H), 7.67 (s, 2H), 7.24−7.23 (dd, 2H), 2.71 (d, 4H), 1.74−1.73 (m, 2H), 1.39−1.28 (m, 32H), 0.93−0.88 (m, 12H), 0.39 (t, 18H). ^{13}C NMR (150 MHz, $CDCl_3$): δ 143.74, 143.48, 140.90, 140.33, 138.59, 137.97, 137.72, 131.02, 126.65, 124.65, 124.31, 122.75, 121.95, 40.70, 40.15, 33.30, 33.03, 32.09, 29.87, 29.03, 26.74, 23.27, 22.85, 14.36, 14.30, −8.13. HRMS (APCI) *m*/*z* calcd for $C_{56}H_{79}S_4Sn_2$ (MH^+) 1117.3111; found 1117.3096.

Synthesis of PBDTBzT-DTffBT and PBDTT-DTffBT. To a 25 mL round-bottom flask was added BDTBzT (BDTT) (0.3 mmol), DTffBT (0.3 mmol), $Pd_2(dba)_3$) (2.8 mg, 0.003 mmol), P(*o*-tol)$_3$ (5.4 mg, 0.018 mmol), anhydrous toluene (10 mL), and anhydrous DMF (2 mL). The mixture was then degassed by argon for 30 min at room temperature. Then the solution was heated to reflux and stirred for 48 h under an argon atmosphere. After cooling to room temperature, the solution was added dropwise into methanol. The precipitate was collected by filtration and extracted by Soxhlet extraction with methanol and hexanes to remove oligomers and catalyst. The residue was dissolved in DCB at 90 °C and then transferred to a chromatographic column containing a short path of silica (80−100 mesh). The column was flushed with DCB. The polymer was precipitated from methanol and dried under vacuum. PBDTBzT-DTffBT. Yield: 64.19%. M_n = 21 987, PDI = 1.84. T_d = 441 °C. ^{1}H NMR (600 MHz, $CDCl_3$): δ 8.35−6.76 (br, 12H), 3.27−2.33 (br, 8H), 2.16−0.35 (m, 76H). PBDTT-DTffBT. Yield: 60.35%. M_n = 23 970, PDI = 1.20. T_d = 431 °C. ^{1}H NMR (600 MHz, $CDCl_3$): δ 8.21−6.72 (br, 8H), 3.19−2.73 (br, 8H), 2.20−0.39 (m, 60H).

■ ASSOCIATED CONTENT

Ⓢ Supporting Information

XRD spectrum; DFT calculations; ^{1}H NMR spectra of monomers and polymers; photovoltaic properties of the

dx.doi.org/10.1021/ma501756p | *Macromolecules* 2014, 47, 7823−7830

polymers with different D/A ratios. This material is available free of charge via the Internet at http://pubs.acs.org.

AUTHOR INFORMATION

Corresponding Author

*E-mail: yangrq@qibebt.ac.cn (R.Y.).

Notes

The authors declare no competing financial interest.

ACKNOWLEDGMENTS

This work was supported by the Ministry of Science and Technology of China (2014CB643501 and 2010DFA52310), the National Natural Science Foundation of China (21274161, 21202181, 21204097, and 51173199), Chinese Academy of Sciences (KGCX2-YW-399 + 9-2), and Qingdao Municipal Science and Technology Program (11-2-4-22-hz).

REFERENCES

(1) Darling, S. B.; You, F. *RSC Adv.* **2013**, *3*, 17633−17648.
(2) Liu, S.; Zhang, K.; Lu, J.; Zhang, J.; Yip, H. L.; Huang, F.; Cao, Y. *J. Am. Chem. Soc.* **2013**, *135*, 15326−15329.
(3) Ye, L.; Zhang, S.; Zhao, W.; Yao, H.; Hou, J. *Chem. Mater.* **2014**, *26*, 3603−3605.
(4) Nguyen, T. L.; Choi, H.; Ko, S.-J.; Uddin, M. A.; Walker, B.; Yum, S.; Jeong, J.-E.; Yun, M. H.; Shin, T.; Hwang, S.; Kim, J. Y.; Woo, H. Y. *Energy Environ. Sci.* **2014**, DOI: 10.1039/c4ee01529k.
(5) He, Z.; Zhong, C.; Su, S.; Xu, M.; Wu, H.; Cao, Y. *Nat. Photonics* **2012**, *6*, 591−595.
(6) Zhang, S.; Ye, L.; Zhao, W.; Liu, D.; Yao, H.; Hou, J. *Macromolecules* **2014**, *47*, 4653−4659.
(7) Jung, E. H.; Jo, W. H. *Energy Environ. Sci.* **2014**, *7*, 650−654.
(8) Guo, X.; Zhou, N.; Lou, S. J.; Smith, J.; Tice, D. B.; Hennek, J. W.; Ortiz, R. P.; Navarrete, J. T. L.; Li, S.; Strzalka, J.; Chen, L. X.; Chang, R. P. H.; Facchetti, A.; Marks, T. J. *Nat. Photonics* **2013**, *7*, 825−833.
(9) Zhang, M.; Guo, X.; Zhang, S.; Hou, J. *Adv. Mater.* **2014**, *26*, 1118−1123.
(10) Huo, L.; Zhang, S.; Guo, X.; Xu, F.; Li, Y.; Hou, J. *Angew. Chem., Int. Ed.* **2011**, *50*, 9697−9702.
(11) Chen, H.-C.; Chen, Y.-H.; Liu, C.-C.; Chien, Y.-C.; Chou, S.-W.; Chou, P.-T. *Chem. Mater.* **2012**, *24*, 4766−4772.
(12) Osaka, I.; Kakara, T.; Takemura, N.; Koganezawa, T.; Takimiya, K. *J. Am. Chem. Soc.* **2013**, *135*, 8834−8837.
(13) Cui, C. H.; Wong, W. Y.; Li, Y. F. *Energy Environ. Sci.* **2014**, *7*, 2276−2284.
(14) Wang, N.; Chen, Z.; Wei, W.; Jiang, Z. *J. Am. Chem. Soc.* **2013**, *135*, 17060−17068.
(15) Cabanetos, C. m.; Labban, A. E.; Bartelt, J. A.; Douglas, J. D.; Mateker, W. R.; Fréchet, J. M. J.; McGehee, M. D.; Beaujuge, P. M. *J. Am. Chem. Soc.* **2013**, *135*, 4656−4659.
(16) Dou, L.; Chen, C.-C.; Yoshimura, K.; Ohya, K.; Chang, W.-H.; Gao, J.; Liu, Y.; Richard, E.; Yang, Y. *Macromolecules* **2013**, *46*, 3384−3390.
(17) Peumans, P.; Yakimov, A.; Forrest, S. R. *J. Appl. Phys.* **2003**, *93*, 3693−3723.
(18) Scharber, M. C.; Mühlbacher, D.; Koppe, M.; Denk, P.; Waldauf, C.; Heeger, A. J.; Brabec, C. J. *Adv. Mater.* **2006**, *18*, 789−794.
(19) Zhou, H.; Yang, L.; Stoneking, S.; You, W. *ACS Appl. Mater. Interfaces* **2010**, *2*, 1377−1383.
(20) Cheng, Y.-J.; Yang, S.-H.; Hsu, C.-S. *Chem. Rev.* **2009**, *109*, 5868−5923.
(21) Mayukh, M.; Jung, I. H.; He, F.; Yu, L. *J. Polym. Sci., Part B: Polym. Phys.* **2012**, *50*, 1057−1070.
(22) Han, L.; Bao, X.; Hu, T.; Du, Z.; Chen, W.; Zhu, D.; Liu, Q.; Sun, M.; Yang, R. *Macromol. Rapid Commun.* **2014**, *35*, 1153−1157.
(23) Chung, H.-S.; Lee, W.-H.; Song, C. E.; Shin, Y.; Kim, J.; Lee, S. K.; Shin, W. S.; Moon, S.-J.; Kang, I.-N. *Macromolecules* **2014**, *47*, 97−105.
(24) Wang, M.; Hu, X.; Liu, P.; Li, W.; Gong, X.; Huang, F.; Cao, Y. *J. Am. Chem. Soc.* **2011**, *133*, 9638−9641.
(25) Son, H. J.; Lu, L.; Chen, W.; Xu, T.; Zheng, T.; Carsten, B.; Strzalka, J.; Darling, S. B.; Chen, L. X.; Yu, L. *Adv. Mater.* **2013**, *25*, 838−843.
(26) Kim, J.-H.; Song, C. E.; Kim, B.; Kang, I.-N.; Shin, W. S.; Hwang, D.-H. *Chem. Mater.* **2014**, *26*, 1234−1242.
(27) Mei, C.-Y.; Liang, L.; Zhao, F.-G.; Wang, J.-T.; Yu, L.-F.; Li, Y.-X.; Li, W.-S. *Macromolecules* **2013**, *46*, 7920−7931.
(28) Chang, C.-Y.; Cheng, Y.-J.; Hung, S.-H.; Wu, J.-S.; Kao, W.-S.; Lee, C.-H.; Hsu, C.-S. *Adv. Mater.* **2012**, *24*, 549−553.
(29) Cheng, Y. J.; Cheng, S. W.; Chang, C. Y.; Kao, W. S.; Liao, M. H.; Hsu, C. S. *Chem. Commun.* **2012**, *48*, 3203−3205.
(30) Hummer, K.; Ambrosch-Draxl, C. *Phys. Rev. B* **2005**, DOI: 10.1103/PhysRevB.71.081202.
(31) Wu, Y.; Li, Z.; Ma, W.; Huang, Y.; Huo, L.; Guo, X.; Zhang, M.; Ade, H.; Hou, J. *Adv. Mater.* **2013**, *25*, 3449−3455.
(32) Zheng, Q.; Jung, B. J.; Sun, J.; Katz, H. E. *J. Am. Chem. Soc.* **2010**, *132*, 5394−5404.
(33) Xu, Y.-X.; Chueh, C.-C.; Yip, H.-L.; Ding, F.-Z.; Li, Y.-X.; Li, C.-Z.; Li, X.; Chen, W.-C.; Jen, A. K.-Y. *Adv. Matter.* **2012**, *24*, 6356−6361.
(34) Perez, M. D.; Borek, C.; Forrest, S. R.; Thompson, M. E. *J. Am. Chem. Soc.* **2009**, *131*, 9281−9286.
(35) Li, Y.; Chang, C.-Y.; Chen, Y.; Song, Y.; Li, C.-Z.; Yip, H.-L.; Jen, A. K. Y.; Li, C. *J. Mater. Chem. C* **2013**, *1*, 7526−7533.
(36) Kularatne, R. S.; Taenzler, F. J.; Magurudeniya, H. D.; Du, J.; Murphy, J. W.; Sheina, E. E.; Gnade, B. E.; Biewer, M. C.; Stefan, M. C. *J. Mater. Chem. A* **2013**, *1*, 15535−15543.
(37) Wu, F.; Zha, D.; Chen, L.; Chen, Y. *J. Polym. Sci., Part A: Polym. Chem.* **2013**, *51*, 1506−1511.
(38) Zhou, H.; Yang, L.; Stuart, A. C.; Price, S. C.; Liu, S.; You, W. *Angew. Chem., Int. Ed.* **2011**, *50*, 2995−2998.
(39) Stuart, A. C.; Tumbleston, J. R.; Zhou, H.; Li, W.; Liu, S.; Ade, H.; You, W. *J. Am. Chem. Soc.* **2013**, *135*, 1806−1815.
(40) Qian, D.; Ye, L.; Zhang, M.; Liang, Y.; Li, L.; Huang, Y.; Guo, X.; Zhang, S.; Tan, Z.; Hou, J. *Macromolecules* **2012**, *45*, 9611−9617.
(41) Guo, X.; Xin, H.; Kim, F. S.; Liyanage, A. D. T.; Jenekhe, S. A.; Watson, M. D. *Macromolecules* **2011**, *44*, 269−277.
(42) Cheng, Y.-J.; Chen, C.-H.; Lin, Y.-S.; Chang, C.-Y.; Hsu, C.-S. *Chem. Mater.* **2011**, *23*, 5068−5075.
(43) Chen, H. Y.; Hou, J.; Hayden, A. E.; Yang, H.; Houk, K. N.; Yang, Y. *Adv. Mater.* **2010**, *22*, 371−375.
(44) Chen, Z.; Cai, P.; Chen, J.; Liu, X.; Zhang, L.; Lan, L.; Peng, J.; Ma, Y.; Cao, Y. *Adv. Mater.* **2014**, *26*, 2586−2591.
(45) Li, Y.; Cao, Y.; Gao, J.; Wang, D.; Yu, G.; Heeger, A. J. *Synth. Met.* **1999**, *99*, 243−248.
(46) Chen, Y.; Du, Z.; Chen, W.; Han, L.; Liu, Q.; Sun, M.; Yang, R. *Synth. Met.* **2014**, *187*, 24−29.
(47) Potscavage, W. J.; Sharma, A.; Kippelen, B. *Acc. Chem. Res.* **2009**, *42*, 1758−1767.
(48) Maurano, A.; Hamilton, R.; Shuttle, C. G.; Ballantyne, A. M.; Nelson, J.; O'Regan, B.; Zhang, W.; McCulloch, I.; Azimi, H.; Morana, M.; Brabec, C. J.; Durrant, J. R. *Adv. Mater.* **2010**, *22*, 4987−4992.
(49) Snaith, H. J.; Greenham, N. C.; Friend, R. H. *Adv. Mater.* **2004**, *16*, 1640−1645.
(50) Liu, J.; Shi, Y.; Yang, Y. *Adv. Funct. Mater.* **2001**, *11*, 420−424.
(51) Du, Z.; Chen, W.; Wen, S.; Qiao, S.; Liu, Q.; Ouyang, D.; Wang, N.; Bao, X.; Yang, R. *ChemSusChem* **2014**, DOI: 10.1002/cssc.201402865.
(52) Liao, H.-C.; Ho, C.-C.; Chang, C.-Y.; Jao, M.-H.; Darling, S. B.; Su, W.-F. *Mater. Today* **2013**, *16*, 326−336.
(53) Chen, W.; Nikiforov, M. P.; Darling, S. B. *Energy Environ. Sci.* **2012**, *5*, 8045−8074.
(54) Ren, G.; Ahmed, E.; Jenekhe, S. A. *Adv. Energy Mater.* **2011**, *1*, 946−953.

(55) Lobez, J. M.; Andrew, T. L.; Bulović, V.; Swager, T. M. *ACS Nano* **2012**, *6*, 3044−3056.
(56) Hu, X.; Yi, C.; Wang, M.; Hsu, C.-H.; Liu, S.; Zhang, K.; Zhong, C.; Huang, F.; Gong, X.; Cao, Y. *Adv. Energy Mater.* **2014**, DOI: 10.1002/aenm.201400378.